THE JOURNAL OF PHYSICAL CHEMISTRY B

Article

pubs.acs.org/JPCB

Exploring Protein Flexibility: Incorporating Structural Ensembles From Crystal Structures and Simulation into Virtual Screening Protocols

David J. Osguthorpe,[†] Woody Sherman,[‡] and Arnold T. Hagler*[,†,§]

[†]Shifa Biomedical, 1 Great Valley Parkway, Suite 8, Malvern, Pennsylvania 19355, United States

[‡]Schrödinger, Inc., 120 West 45th Street, 17th Floor, New York, New York 10036, United States

[§]Department of Chemistry, University of Massachusetts, 701 Lederle Graduate Research Tower, 710 North Pleasant Street, Amherst, Massachusetts 01003-9336, United States

Supporting Information

ABSTRACT: The capacity of proteins to adapt their structure in response to various perturbations including covalent modifications, and interactions with ligands and other proteins plays a key role in biological processes. Here, we explore the ability of molecular dynamics (MD), replica exchange molecular dynamics (REMD), and a library of structures of crystal-ligand complexes, to sample the protein conformational landscape and especially the accessible ligand binding site geometry. The extent of conformational space sampled is measured by the diversity of the shapes of the ligand binding sites. Since our focus here is the effect of this plasticity on the ability to identify active compounds through virtual screening, we use the structures generated by these techniques to generate a small ensemble for further docking studies, using binding site shape hierarchical clustering to determine four structures for each ensemble. These are then assessed for their capacity to optimize enrichment and diversity in docking. We test these protocols on three different receptors: androgen receptor (AR), HIV protease, and CDK2. We show that REMD enhances structural sampling slightly as compared both to MD, and the distortions induced by ligand binding as reflected in the crystal structures. The improved sampling of the simulation methods does not translate directly into improved docking performance, however. The ensemble approach did improve enrichment and diversity, and the ensemble derived from the crystal structures performed somewhat better than those derived from the simulations.

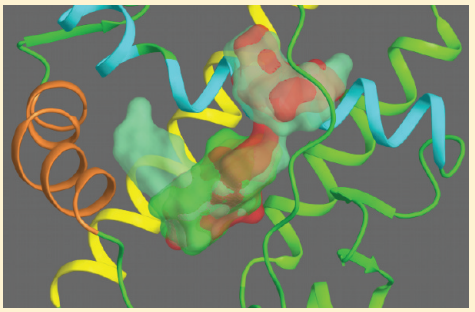

INTRODUCTION

In a previous paper we investigated the use of a small ensemble of protein structures based on the diversity of binding site shapes to account for protein flexibility in docking. We found that the use of four diverse structures indeed improves consistency in results, database enrichment rates, and diversity of the hits obtained from docking. The studies were performed on crystal structures of HIV-1 protease and CDK2 and also on a structural ensemble generated from molecular dynamics (MD) simulations of androgen receptor (AR). We found that the MD ensemble of structures produced improved docking enrichment over a single crystal structure, consistent with the findings from the crystal structure ensembles. However, using multiple MD structures for AR did not improve results as significantly as using multiple crystal structures did for the HIV-1 protease and CDK2 systems and, perhaps surprisingly, the diversity of shapes was smaller than that from the different crystal structures.

In this paper we apply MD to the same three systems (HIV-1 protease, CDK2, and AR) and study more rigorous sampling through the use of replica exchange molecular dynamics (REMD).[1] The diversity of ligand binding site (LBS) shapes and the enrichment achieved from docking into the ensemble of structures obtained in these studies are compared to those obtained from the previous crystal studies. In addition, we generated an ensemble of ligand binding shapes from the universe of AR-ligand crystal structures and carried out the same analysis of docking results using these.

Our objective is twofold. First, we explore whether the use of MD to improve enrichment through generating diverse structures is a generally applicable approach, or if the AR results were in some way unique to that system. Second, we investigate whether the apparently limited sampling of lBS structure by the MD was due to the use of a limited portion of a single trajectory or is also a general phenomenon. REMD was performed to improve the sampling over standard MD with the hopes that the additional sampling from the single initial crystal structure would improve the virtual screening results. In addition, we performed an LBS SiteMap clustering of the REMD "trajectories" as well as

Special Issue: Harold A. Scheraga Festschrift

Received: January 12, 2012
Revised: March 9, 2012
Published: March 16, 2012

   dx.doi.org/10.1021/jp3003992 | J. Phys. Chem. B 2012, 116, 6952–6959

on 44 AR crystal structures to have a complete set of the three systems. The results of docking into the small ensemble of diverse LBS structures resulting from this clustering was then analyzed to ascertain whether the enrichment and diversity achieved with REMD is comparable or perhaps superior to that achieved from crystal structures or MD.

METHODS

Crystal Structures and Initial Preparation. We searched the PDB for AR ligand binding domain (LBD) structures and selected 44 for clustering. The protein structures were prepared using the Schrodinger Protein Preparation Wizard (PrepWizard).[2] This preparation protocol added hydrogens, built side chains and loops with missing atoms, determined the optimal protonation states for ionizable residues, optimized the hydrogen-bonding network, and performed a restrained minimization to obtain the final structure for running docking or simulations.

Choice of Systems for MD Studies. As noted in the Introduction, we studied the three systems (HIV-1 protease, CDK2, and AR) used previously to assess database enrichments and diversity of retrieved ligands in ensemble docking. For HIV-1 protease, we used the 1EBZ structure from the PDB for the MD since 1EBZ was the representative structure of the cluster with the largest number of structures from our previous clustering of 135 HIV-1 protease structures.[3] Two CDK2 structures were chosen, one with cyclin bound and another without cyclin bound. These two forms have significant structural changes due to refolding of the sections of the CDK2 structure involved in cyclin binding. Our previous clustering of 92 structures[3] separated these two forms into different clusters, and we chose the noncyclin bound structure as the cluster representative from the largest cluster of noncyclin bound structures (1W0X) and the cluster representative of the single cyclin bound cluster (1OI9) for the MD simulations. For AR we used the 1T63 AR-DHT complex we investigated previously.[4]

Preparation of Protein Systems for MD and REMD. The PDB structures were prepared with the Schrodinger PrepWizard utility as described above. The prepared systems were solvated using the System Builder program of the Desmond suite with a dodecahedral solvent box and a solvent buffer extending 10 Å beyond the protein in all directions. The systems were neutralized with counterions, which entailed adding different numbers of Na^+ or Cl^- ions to each system. Four Cl^- ions were added for HIV-1 protease, and five and two Cl^- ions were added for apo- and cyclin-bound CDK2, respectively. For the AR structure, we used the existing prepared starting structure for the solvated MD studies as in our previously published AR work.[4]

Molecular Dynamics. MD simulations were carried out using the Desmond suite[5] with long-range electrostatic interactions computed using a smooth particle-mesh Ewald (PME) approximation[6] with a cutoff radius of 9.0 Å for the transition between the particle−particle and particle−grid calculations. van der Waals (vdW) interactions were truncated at 9.0 Å. Dodecahedral periodic boundary conditions were used for all simulations. MD steps were integrated using a two time-step algorithm, with 2 fs steps for bonded and short-range interactions within the 9.0 Å cutoff and 10 fs for long-range nonbonded interactions. The system was relaxed using a protocol consisting of an initial minimization, MD for 20 ps at 0.1 K, MD for 20 ps at 310 K, both with restraints of 250 kcal/mol/Å^2 on all heavy atoms using the Berendsen[7] thermostat, followed by 100 ps with restraints of 2.5 kcal/mol/Å^2 performed using 1 fs short-range and 5 fs long-range timesteps to reduce numerical issues with large initial forces. This was followed by 100 ps using the NPT ensemble and Berendsen thermostat and barostat and 100 ps Nose−Hoover thermostat and Martyna−Tuckerman−Klein barostat.[8] This was extended to 1 ns with no restraints. The production MD simulations were carried out at 310 K using the NVT ensemble with a Nose−Hoover thermostat.[9,10] Trajectories were run for 5 ns, with the equilibration being carried out over the first nanosecond and analysis carried out on the final four nanoseconds.

Replica Exchange Molecular Dynamics. REMD is a procedure for improving sampling by performing multiple simulations of the same system at different temperatures in parallel.[1,11−13] At fixed time intervals, a so-called "exchange" is attempted in which both the coordinates and velocities from a pair of adjacent temperature simulations are swapped. A Metropolis criterion[14] is used to determine whether the exchange should be accepted (eq 1).

$$P(x|x') = \left\{ \frac{1 \text{ for } \Delta \le 0}{\exp(-\Delta) \text{ for } \Delta > 0} \right\}$$

$$\text{where} \quad \Delta = (\beta - \beta')(V(x') - V(x))$$

$$\beta = 1/kT, \quad \beta = 1/kT'$$

x and x' are the confgurations at T and T', respectively

V and V' are the potential energies of the two configurations (1)

This procedure guarantees that in the long run for each simulation in the REMD set, averages over the trajectory are thermodynamically valid. The ability for configurations from higher temperatures to swap to lower temperatures improves the sampling of configurations at that temperature compared to performing a standard MD trajectory.

The rate at which exchanges are accepted should be similar for each trajectory and allow a reasonable residence time for an exchanged structure at that temperature (around 10 ns). The temperature differences needed to achieve this can be estimated using an algorithm published by Patriksson.[15] This algorithm was used to determine the temperature distribution in this work. Given our initial choice of a 100° temperature range, from 298 to 398 K, the total number of replicas was determined as a function of the system size (i.e., number of atoms). The 100° temperature range was intended to improve sampling but not to introduce unfolding at the higher temperatures. Forty-five replicas were required for HIV-1 protease, while 55 and 53 replicas were used for the two CDK2 systems, and AR required 44 replicas. REMD simulations at each temperature were performed for 3 ns using the Desmond program suite[5] with the same methods as described above for the MD, resulting in approximately 150 ns of total simulation time for each system.

Ligand Binding Site Shape Clustering. As in our previous study,[3] the program SiteMap[16,17] was used to compute the binding site shape for each receptor structure. Structures were superimposed using Cα atoms of common residues within 8 Å of the ligands. The volume overlap of the sites for each pair of structures was computed to create the volume overlap matrix. Hierarchical clustering was applied to this matrix using average linkage to create a clustering order. A cluster partitioning of four was chosen as a balance between time and completeness of

dx.doi.org/10.1021/jp3003992 | J. Phys. Chem. B 2012, 116, 6952−6959

sampling. For each partition, the cluster representative was determined to realize a set of diverse binding site shapes.

Ligand Data Sets. The DUD data set[18] was chosen as the test data set to provide active and decoy ligands. This included 52 unique active ligands and 1884 decoys for HIV-1 protease and 49 unique active ligands and 1778 decoys for CDK2. For AR, the set included 73 active ligands and 2627 decoys.

Docking. As in our previous work,[3] the Glide SP algorithm was used for docking[19,20] with the final scoring using the GlideScore. The GlideScore has empirical terms to account for desolvation effects and special reward terms to account for interactions that are difficult to accurately compute with force fields, such as pi-pi and pi-cation interactions.

Database Enrichment and Diversity Assessment. The enrichment factor (EF) was computed using eq 2:

$$\mathrm{EF} = F_a/F_d \tag{2}$$

where F_a is the fraction of actives found, and F_d is the fraction of the database sampled. In this study, as previously, we have calculated enrichment factors for the actives found in the top scoring 1% and 4% of the total compounds docked (denoted EF(1%) and EF(4%), respectively).

The diversity of ligands selected was computed as follows: The MACCs fingerprints[21] of the active ligands were determined, and hierarchical clustering was performed on the matrix of pair similarities determined using the Tanimoto metric using the program Canvas.[22] From inspection of the resulting clustering of all actives in each DUD ligand data set (Figure 1 shows the clustering of AR, with those of HIV and CDK2 in the Supporting Information Figures S4 and S5), a clustering level of 0.7 similarity was chosen as separating the active ligands into different chemotypes. For each cluster representative, after docking, the actives in the 1% ligands were clustered, and the number of clusters at the 0.7 level was determined. This number of clusters gives an estimate of the diversity of the hits found from docking.

RESULTS

Molecular Dynamics. In order to assess the ability of MD to sample the accessible configuration space of the LBS, we carried out standard MD and REMD simulations of AR, CDK2,

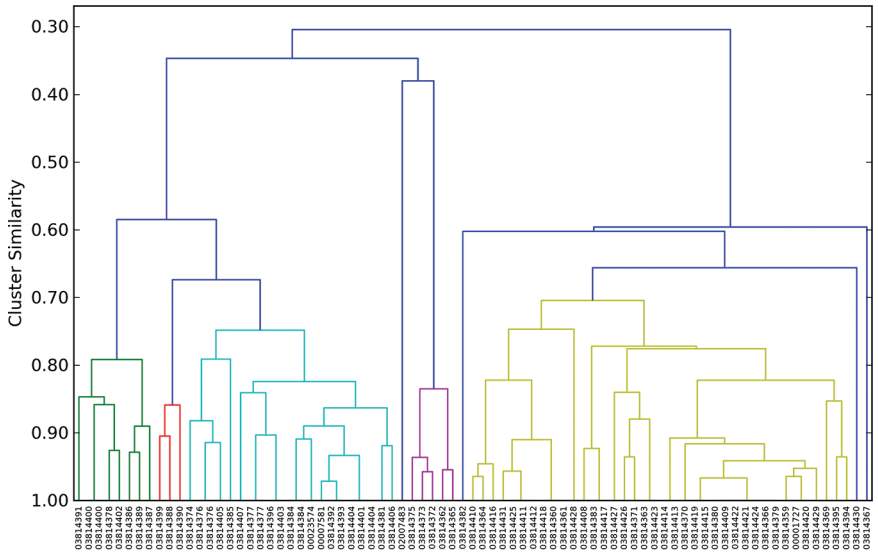

Figure 1. Dendrogram of clustering the 74 active ligands of the AR DUD data set by their MACCs fingerprints, defining clusters at the 0.7 level and using the same color for the members of each cluster and blue for singleton clusters. The *x*-axis is the ZINC ID numbers.

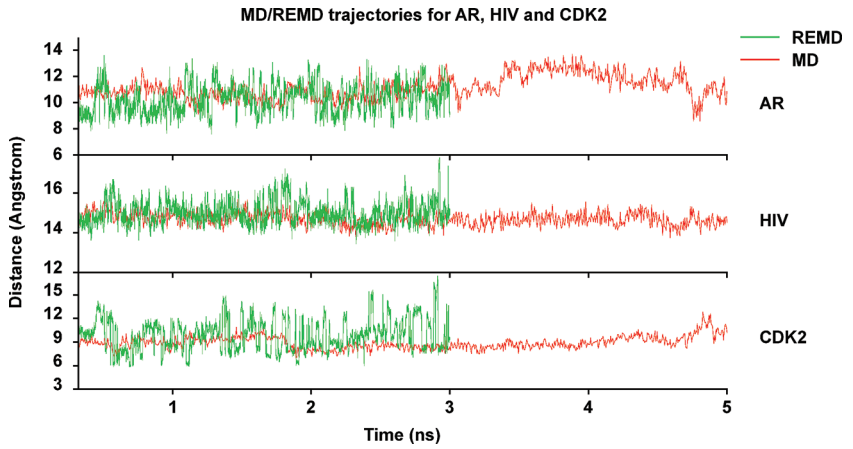

Figure 2. Trajectory of residue−residue distances spanning the binding sites for the AR, HIV-1 protease, and CDK2 MD (red) and REMD (green) simulations. The AR trajectory is characterized by the distance between the Gln 711 side chain amide nitrogen and the Met 895 sulfur. The HIV-1 protease trajectory corresponds to the Val 82−Val 182 side chain distance, and the CDK2 trajectory corresponds to the Tyr 15−Asn 132 side chain distance.

dx.doi.org/10.1021/jp3003992 | J. Phys. Chem. B 2012, 116, 6952−6959

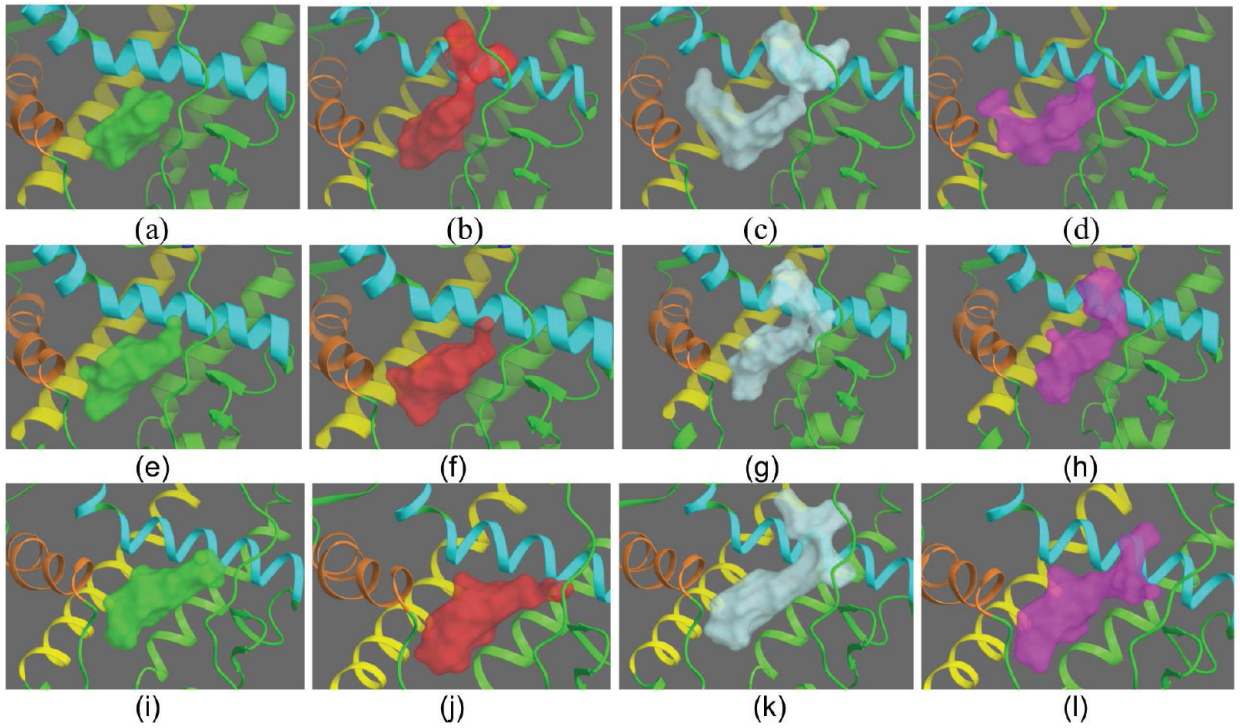

Figure 3. Active site shapes for the AR from crystal structures, MD and REMD. The four crystal structure cluster representatives of AR are given in panels a−d, the four cluster representatives from MD are given in structures e−h, while the four cluster representatives from REMD are given in i−l. Helix 3 of AR, which runs roughly vertically in front of the LBS, has been removed from view for clarity.

and HIV-1 protease. The MD and REMD trajectories of the distance between residues roughly characterizing the LBS width are given in Figure 2 for the three proteins. As can be seen from the figure, the distances visited during the trajectories for all three systems span a greater range for the REMD, as might be expected from its superior sampling ability[1,11−13] even though the REMD trajectories are slightly shorter. This is especially true for the HIV-1 protease and CDK2 systems, while in the case of AR, the MD eventually visits almost the whole span of distances, albeit briefly in some cases.

Exploration of LBS Shapes By MD versus Crystal Structures. The structures obtained from the three sources (crystal, MD, and REMD) were then used to generate structural ensembles for virtual screening through hierarchical clustering. The resulting representative structures from MD and REMD were then compared with those obtained from the crystal structures.[3] A sense of the LBS plasticity can be obtained by examining the LBS volumes of the cluster representatives sampled by the different methods. These are given for AR in Figure 3 and for CDK2 and HIV-1 protease in the Supporting Information. As can be seen in Figure 3, the crystal structures appear to show a greater diversity of volumetric shape than the MD structures, with four distinctly different shapes. The MD structures show essentially two different shapes as opposed to the greater variation in the crystal structures. This is consistent with the results in our previous study, where the volume overlap matrices indicated that the crystal complexes of HIV-1 protease and CDK2 sampled the accessible LBS volumetric space more effectively than the (limited) MD did for AR[3] (and was one of the motivating factors for this study).The REMD cluster representatives are distinctly different from the crystal and MD volumes but show some similarities in overall shape, with Figure 3k (cyan shaded) showing features similar to those in panel b from the crystal and MD (h), although as seen from the overlap matrix given below, the similarity of features does not necessarily equate to a global volume similarity.

Overlap Volumes of Representative AR Structures. The greater diversity of the crystal shapes is further demonstrated by the normalized overlap volume matrix for the crystal and MD cluster representatives of AR (Table 1). The overlap matrix of the representative structures from MD confirms that the two pairs of structures are more similar to each other than to the other pair (e−f, g−h, shaded yellow and light blue) with the smallest similarity between the two pairs being 0.55.

By comparison, the least similar structures from the crystals have an overlap volume of 0.45. The average normalized overlap volume for all pairs is 0.64 for the MD cluster representatives versus 0.57 for the crystal, showing the crystal structure volumes sample a larger binding site structural space, on average, than the MD volumes in this system. The average of the normalized overlap matrix of the four cluster representatives from the REMD sampling of AR is 0.60, which is somewhat lower than the MD average (0.64), indicating that REMD has increased the diversity of volumes slightly, but still does not achieve the sampling of LBS volume induced by different ligands (average crystal overlap volume 0.57).

LBS Volumetric Sampling of HIV-1 Protease and CDK2 Yields Different Trends Then AR. To assess the generality of this result, we compare the sampling achieved by the three methods for the HIV-1 protease and CDK2 systems as well. Figures of the representative structures arising from the clustering of the crystal and dynamic trajectories are given in the Supporting Information (Figures S1 and S2). Figure S1 shows that the HIV-1 protease REMD shapes are more varied than the MD, with more open space in most of the representatives, suggesting that the REMD has searched more of the conformational space. This is confirmed by the overlap matrix for the HIV-1 protease representative structures, as seen in Table 2. In this system, unlike the behavior for AR, we see that a greater sampling efficiency is indeed

dx.doi.org/10.1021/jp3003992 | J. Phys. Chem. B 2012, 116, 6952−6959

Table 1. Normalized Overlap Volume Matrix of the Four Crystal Cluster Representatives for AR, the Four MD Cluster Representatives for AR, and the Four REMD Cluster Representatives for AR 310 K[a]

Crystal												
	1T74	2AMA	2AXA	2HVC								
1T74	1.00	0.69	0.45	0.66								
2AMA	0.69	1.00	0.56	0.57								
2AXA	0.45	0.56	1.00	0.51								
2HVC	0.66	0.57	0.51	1.00								
MD						e	f	g	h			
e	0.70	0.57	0.41	0.57		1.00	0.71	0.59	0.66			
f	0.71	0.59	0.46	0.60		0.71	1.00	0.55	0.61			
g	0.57	0.57	0.48	0.46		0.59	0.55	1.00	0.69			
h	0.56	0.55	0.49	0.46		0.66	0.61	0.69	1.00			
REMD										i	j	k	l
i	0.63	0.57	0.38	0.50		0.64	0.64	0.57	0.54	1.00	0.70	0.60	0.64
j	0.70	0.59	0.38	0.53		0.69	0.70	0.54	0.53	0.70	1.00	0.58	0.55
k	0.56	0.53	0.45	0.44		0.57	0.57	0.59	0.56	0.60	0.58	1.00	0.50
l	0.51	0.42	0.29	0.41		0.53	0.51	0.50	0.41	0.64	0.55	0.50	1.00

[a]Cross-normalized overlap volumes between the crystal, MD, and REMD shapes are shaded green.

Table 2. Normalized Overlap Volume Matrix of the Four Crystal Cluster Representatives for HIV, the Four MD Cluster Representatives for HIV-1 Protease, and the Four REMD Cluster Representatives for HIV-1 Protease 310 K[a]

Crystal												
	1EBZ	1HVS	1XL2	3AID								
1EBZ	1.00	0.56	0.35	0.39								
1HVS	0.56	1.00	0.38	0.40								
1XL2	0.35	0.38	1.00	0.37								
3AID	0.39	0.40	0.37	1.00								
MD						e	f	g	h			
e	0.29	0.29	0.25	0.30		1.00	0.38	0.43	0.41			
f	0.38	0.33	0.32	0.30		0.38	1.00	0.42	0.46			
g	0.26	0.27	0.23	0.28		0.43	0.42	1.00	0.50			
h	0.29	0.29	0.25	0.27		0.41	0.46	0.50	1.00			
REMD										i	j	k	l
i	0.36	0.37	0.30	0.32		0.35	0.36	0.35	0.36	1.00	0.24	0.33	0.26
j	0.24	0.22	0.24	0.26		0.34	0.37	0.38	0.34	0.24	1.00	0.37	0.35
k	0.37	0.38	0.28	0.39		0.34	0.28	0.33	0.29	0.33	0.37	1.00	0.37
l	0.15	0.19	0.24	0.24		0.27	0.34	0.29	0.30	0.26	0.35	0.37	1.00

[a]Cross-normalized overlap volumes between the crystal, MD, and REMD shapes are shaded green.

achieved by the REMD method, than by either the crystal structures or the MD, consistent with the trend seen in the distance trajectory in Figure 1. Thus the average of the normalized overlap volume matrices is 0.41 and 0.43, and 0.32 for the crystal, MD, and REMD sampling, respectively, reflecting a significantly more extensive sampling by the REMD method.

Comparison of LBS Volumes Obtained from Different Methods. As might be expected, at least for the dynamic

dx.doi.org/10.1021/jp3003992 | J. Phys. Chem. B 2012, 116, 6952−6959

Table 3. Normalized Overlap Volume Matrix of the Four Crystal Cluster Representatives for CDK2, the Four MD Cluster Representatives for CDK2, and the Four REMD Cluster Representatives for CDK2 310 K[a]

Crystal				
	1OI9	2BHE	1GZ8	1W0X
1OI9	1.00	0.46	0.40	0.49
2BHE	0.46	1.00	0.38	0.52
1GZ8	0.40	0.38	1.00	0.50
1W0X	0.49	0.52	0.50	1.00

MD					e	f	g	h
e	0.36	0.32	0.45	0.44	1.00	0.37	0.31	0.29
f	0.32	0.26	0.38	0.35	0.37	1.00	0.41	0.39
g	0.28	0.27	0.30	0.31	0.31	0.41	1.00	0.43
h	0.52	0.41	0.37	0.45	0.29	0.39	0.43	1.00

REMD									i	j	k	l
i	0.51	0.43	0.33	0.42	0.30	0.35	0.37	0.50	1.00	0.49	0.41	0.38
j	0.47	0.39	0.40	0.42	0.31	0.37	0.28	0.51	0.49	1.00	0.37	0.40
k	0.44	0.43	0.44	0.55	0.49	0.35	0.31	0.43	0.41	0.37	1.00	0.35
l	0.37	0.28	0.46	0.37	0.46	0.47	0.40	0.38	0.38	0.40	0.35	1.00

[a]Cross-normalized overlap volumes between the crystal, MD, and REMD shapes are shaded green.

methods, which trace the trajectory of a single structure, the "cross" overlap matrices between volumes obtained from different methods tend to show a greater variation in volumes than those from any of the individual techniques. Thus, for example, the overlap between the first representative structure from the crystal with the fourth REMD structure is only 0.15, lower than any of the overlaps within a set. The average overlaps for representative structures from the HIV-1 protease crystal clustering with those from MD is 0.29 and for the crystal REMD and MD REMD, 0.28 and 0.33, respectively. This trend is also observed in the AR structures.

CDK2−Cyclin versus Noncyclin Bound. Finally, in Table 3, we give the overlap matrices for the CDK2 system. The CDK2 structures separate globally into two basic classes: the cyclin and noncyclin bound structures. In the crystal, the former structures assemble into a single cluster, while the noncyclin structures are spread among the remaining three clusters with the exception of two noncyclin structures, which appear in the cyclin bound cluster (Figure S3). Similar results are found in the distribution of structures from the MD. Namely, all cyclin bound structures are found in a single cluster, which interestingly contains two of the 800 noncyclin structures that are visited along the MD trajectory. The REMD results are similar in that, again, all cyclin bound structures along the REMD "trajectory" group together in a single cluster. However, in this case, 103 of the 800 noncyclin structures sampled in the REMD simulation group with the cyclin bound cluster. The excursion of the noncyclin structures into the cyclin bound configuration space is consistent with the enhanced ability of REMD to sample the energy landscape.

Simulations Sample Greater Volume Diversity than Crystal Structures in CDK2. As in the case of the AR and HIV-1 protease systems, another measure of the plasticity of the protein sampled by the different techniques is the similarity of the LBS volumes of the representative structures. Here the results differ slightly from what might be expected from the nature of the clustering and from the results of the AR and HIV-1 protease systems. In this case, as can be seen from the normalized overlap volumes in Table 3, both the MD and REMD simulations visit more diverse volumes than induced by the ligands in the crystal structures, but in this case the MD simulations also span slightly more "volume space" than the REMD. This is reflected in the average overlap volumes of 0.46, 0.37, and 0.40 for the crystal, MD, and REMD, respectively.

Does the Ensemble of Structures Obtained from Simulations Improve Enrichment over Docking into a Single Structure? The purpose of these studies is to develop methods for improving enrichment in virtual screening campaigns. Thus, the bottom line is whether docking into small ensembles obtained from simulations of dynamics improve enrichment over docking into a single structure, and, second, how this enrichment compares with that achieved with ensembles derived from crystal structures.

In Table 4 we show the results of docking into the individual four cluster representatives obtained from crystal structures, MD, and REMD for the HIV-1 protease system. The enrichment achieved by exploiting the ensemble is better than or equal to (in the case of MD) the average enrichment, which would be achieved by taking the same number of hits from the single structures. For example, 13 actives are found in the combined hits from the top 1% of hits from each representative structure of the crystal, while, if we just took the top 4% of the hits from individual structures, we would only recover ∼10 actives on average. As noted previously,[3] there are individual structures, for example, representative structure 2 in the case of HIV-1 protease, which would yield a greater enrichment than

dx.doi.org/10.1021/jp3003992 | J. Phys. Chem. B 2012, 116, 6952−6959

Table 4. HIV-1 Protease Active Ligands and Decoy Ligands Docking to Four Representative Structures from Crystal, MD and REMD[a]

cluster representative		count of active ligands top 19 (1%)[b]	count of active ligands top 76 (4%)	enrichment factor top 19 (1%)	enrichment factor top 76 (4%)	diversity of actives top 19 (1%)	diversity of actives top 76 (4%)
crystal	1	6 (6)	10	12	4.8	3	5
	2	10 (5)	16	19	7.7	5	6
	3	3 (0)	6	6	2.9	2	4
	4	7 (2)	9	13	4.3	3	5
ensemble		13	10.3[c]	6.3	4.9	6	5.0
MD	1	8 (2)	13	15	6.3	4	6
	2	2 (0)	8	3.8	3.8	1	3
	3	6 (1)	12	12	5.8	1	4
	4	7 (7)	8	13	3.8	3	3
ensemble		10	10.3	4.8	4.9	4	4.0
REMD	1	6 (6)	11	12	5.3	1	3
	2	8 (6)	17	15	8.2	5	6
	3	2 (0)	6	3.9	2.9	2	2
	4	4 (1)	8	7.7	3.8	2	3
ensemble		13	10.5	6.3	5.0	5	3.5

[a]Active ligand counts, enrichment factors, and diversity for each structure at the 1% and 4% level. [b]Additional unique ligand count shown in brackets; these are the ligands of the current structure that are different from any active ligand of structures before this structure. [c]This is the average over the active ligands recovered in the top 4% of hits.

the ensemble. Unfortunately, there is no clear way to choose a priori the best structure for docking.

Diversity of Hits. As noted above, not only are we interested in optimizing the recovery of actives in a virtual screening campaign, but equally important, we would also like to find a diverse set of hits on which to base further drug design efforts. The diversity of ligands is measured by the number of clusters (~chemotypes) found at the 0.7 similarity level from a hierarchical clustering of the ligands, as described in the Methods section. As with enrichment of HIV-1 protease hits, we see from Table 4 that the ensemble produces greater diversity than is achieved by docking into single structures, with the exception of the MD simulation. Again, one could achieve similar diversity from a single structure if one were fortunate enough to pick the best structure in which to dock.

Summary of Enrichment and Diversity Comparison for the Three Systems. The results for all three systems studied here are summarized in Table 5, and the detailed tables for AR and CDK2 are given in the Supporting Information (Tables S1 and S2). As we see from Table 5, in all cases, the ensemble produces a better enrichment and greater diversity of hits than from the same number of compounds taken from docking into a single structure for the crystal structures. For example, the ensemble docking yields enrichment factors of 13.0, 6.3, and 9.1 for the crystal systems of AR, HIV, and CDK2, respectively, while the average of the comparable enrichment factors for docking into single structures for the same systems is 9.7, 4.9, and 6.3, respectively. The diversity, as measured by the number of clusters/"chemotypes" recovered from the ensemble, is also superior (4, 6, and 11) as compared to the average crystal values (3.5, 5.0, and 7.0), respectively. Similar results are found from the structures derived from REMD, with the exception of AR. The MD results do not follow this trend with both the AR and HIV-1 protease systems showing greater or equal enrichment from docking into a single structure, and the average diversity achieved is also greater in the top 4% of the hits from single structures, as opposed to the combined top 1% of each of the individual representative structures. In CDK2, docking into the ensemble again produces better enrichment and diversity than the single structures.

DISCUSSION AND CONCLUSIONS

We have shown that MD and REMD simulation techniques can be used to generate diverse structures that may be exploited to improve database enrichment and diversity in virtual screening campaigns as compared with the use of a single receptor structure. Furthermore, a procedure was described to select an ensemble of structures based on the diversity of the binding site shapes. The ensemble selection is an unbiased procedure based on hierarchical clustering to select diverse binding site shapes.

The results presented here show that structures generated from MD and REMD simulations can be used in docking studies and provide significant enrichment and diversity of hits. In all three systems, docking into structures taken from MD and REMD yield good enrichment of actives, ranging from 3.8-fold improvement over random in the case of MD structures of CDK2 to 9.7-fold over random in AR, when analyzing the top 4% of the virtual screening hits. However, when many crystal structures are available, docking into an

Table 5. Comparison of Ensemble 1% Results with Average of 4% Results for Crystal, MD and REMD Studies of AR, HIV-1 Protease and CDK2

system		count of active ligands ensemble 1%[a]	count of active ligands average 4%[b]	enrichment factor ensemble 1%[c]	enrichment factor average 4%[d]	diversity of actives ensemble 1%[e]	diversity of actives average 4%[f]
AR	crystal	39	28.8	13	9.7	4	3.5
	MD	25	27.0	8.5	9.0	3	2.3
	REMD	20	28.5	6.8	9.7	2	2.3
HIV	crystal	13	10.3	6.3	4.9	6	5.0
	MD	10	10.3	4.8	4.9	2	4.0
	REMD	13	10.5	6.3	5.0	5	3.5
CDK2	crystal	18	12.5	9.1	6.3	11	7.0
	MD	12	7.8	6.1	3.9	8	5.3
	REMD	12	7.5	6.1	3.8	8	5.5

[a]Count of unique active ligands from all four structures at the 1% level. [b]Average of active ligand count for the four structures at the 4% level. [c]EF computed using the count of unique active ligands from all four structures at the 1% level. [d]Average of the EF computed at the 4% level for each structure. [e]Diversity computed using the unique active ligands from all four structures at the 1% level. [f]Average of the diversity computed at the 4% level for each structure.

dx.doi.org/10.1021/jp3003992 | J. Phys. Chem. B 2012, 116, 6952−6959

ensemble of binding site shape diverse crystal structures yields better enrichment and diversity of active ligands than docking into structures derived from simulations. Thus, one should use crystal structures if enough structures are available to achieve binding site diversity sufficient to accommodate the diversity of actives sought. The results from AR also confirm the conclusion drawn previously that docking into a small ensemble of representative crystal structures will yield better enrichment and diversity than docking into a single structure.

The value of using REMD versus MD for the generation of receptor structures is not clear from the limited studies performed here. In HIV-1 protease, greater enrichment is achieved by the REMD ensemble docking, whereas in CDK2 there is no difference in enrichment between MD and REMD. In AR, equal or better enrichment is achieved by docking into any of the single representative structures from the simulation techniques than exploiting the top 1% of each structure in the ensemble. The reason for this is the subject of further study.

It was hypothesized that the relatively greater effectiveness of the crystal structures in the CDK2 and HIV-1 protease to yield enrichment in docking over the MD structures of AR was due to the limited sampling in the 1 ns portion of the MD trajectory exploited. Here, we employed REMD simulations to test this hypothesis. As seen from the resulting docking studies carried out in all three systems, the improved sampling afforded by the REMD did not translate into improved enrichment or diversity. The reason for this remains to be elucidated. The LBS volume overlap matrices of the REMD with the crystal structures indicate that the simulations sample regions of LBS volumes that are not sampled by the crystal-ligand systems. This raises the question as to whether the REMD energy surface is adequately true to the actual energy surface of the protein ligand system, leading to slight artifactual excursions in the configuration space of the protein. That these deviations are not too extreme is demonstrated by the success of the structures in the trajectory to yield significant enrichment in docking, albeit not quite as competently as the crystal structures.

Perhaps a more plausible explanation is that binding site diversity alone is not a sufficient descriptor to determine the best structures to use for virtual screening. An extreme scenario can be constructed where a very diverse structure results from the binding site completely collapsing, yielding a "diverse" structure that would not accommodate any active compounds. While such an extreme situation was not encountered in the work presented here, more subtle situations may exist with side chains moving into positions that create diverse shapes that cannot accommodate active ligands. One possible solution would be to generate a diverse ensemble of structures under the constraint that certain other characteristics of the binding site are maintained, such as total volume, degree of enclosure, etc. Such a study is beyond the scope of the work presented here and will be the focus of future studies.

■ ASSOCIATED CONTENT

Supporting Information

Description: This lists the PDB IDs for the AR crystal clustering, figures of the active site shapes for HIV and CDK2 from crystal, MD and REMD structures clustering, a dendrogram of the CDK2 crystal clustering, tables of detailed results for active ligand counts, enrichment factors and diversity estimates for docking to each individual crystal, MD and REMD cluster representative for AR, CDK2, and HIV, and a dendrogram of HIV and CDK2 active ligand clustering using MACCs fingerprints. The additional figures and tables referenced in the paper are also included. This material is available free of charge via the Internet at http://pubs.acs.org.

■ AUTHOR INFORMATION

Corresponding Author

*Address: Dept. of Chemistry, University of Massachusetts, P.O. Box 12067, La Jolla, CA 92039. Phone: 619 379-9768; e-mail: athagler@gmail.com.

Notes

The authors declare no competing financial interest.

■ ACKNOWLEDGMENTS

This work was supported by the National Institutes of Health Grant R43 CA132538, and the National Science Foundation Grant CNS 0551500. A.T.H. would like to acknowledge Prof. Harold Scheraga, a mentor and friend for many years.

■ REFERENCES

(1) Sugita, Y.; Okamoto, Y. *Chem. Phys. Lett.* **1999**, *314*, 141−151.
(2) Maestro, version 9.2; Schrödinger, LLC: New York, 2011.
(3) Osguthorpe, D. J.; Hagler, A. T.; Sherman, W. *Chem. Biol. Drug Des.* **2012**, in press.
(4) Osguthorpe, D. J.; Hagler, A. T. *Biochemistry* **2011**, *50*, 4105−4113.
(5) Bowers, K. J.; Chow, E.; Huafeng, X.; Dror, R. O.; Eastwood, M. P.; Gregersen, B. A.; Klepeis, J. L.; Kolossváry, I.; Moraes, M. A.; Sacerdoti, F. D.; Salmon, J. K.; Yibing, S.; Shaw, D. E. Proceedings of the ACM/IEEE Conference on Supercomputing (SC06), Tampa, FL, November 11−17, 2006.
(6) Darden, T.; York, D.; Pedersen, L. *J. Chem. Phys.* **1993**, *98*, 10089−10092.
(7) Berendsen, H. J. C.; Postma, J. P. M; van Gunsteren, W. F.; DiNola, A.; Haak, J. R. *J. Chem. Phys.* **1984**, *81*, 3684−3690.
(8) Martyna, G. J.; Tuckerman, M. E.; Tobias, D. J.; Klein, M. L. *Mol. Phys.* **1996**, *87*, 1117−1157.
(9) Nose, S. *J. Chem. Phys.* **1984**, *81*, 511−519.
(10) Hoover, W. G. *Phys. Rev. A* **1985**, *31*, 1695−1697.
(11) Hukushima, K.; Nemoto, K. *J. Phys. Soc. Jpn.* **1996**, *65*, 1604−1608.
(12) Garcia, A. E.; Sanbonmatsu, K. Y. *Proteins* **2001**, *42*, 345−354.
(13) Garcia, A. E.; Onuchic, J. N. *Proc. Natl. Acad. Sci. U.S.A.* **2003**, *100*, 13898−13903.
(14) Metropolis, N.; Ulam, S. *J. Am. Stat. Assoc.* **1949**, *44*, 335−341.
(15) Patriksson, A.; van der Spoel, D. *Phys. Chem. Chem. Phys.* **2008**, *10*, 2073−2077.
(16) Tom, H. *Chem. Biol. Drug Des.* **2007**, *69*, 146−148.
(17) Halgren, T. A. *J. Chem. Inf. Model.* **2009**, *49*, 377−389.
(18) Huang, N.; Shoichet, B. K.; Irwin, J. J. *J. Med. Chem.* **2006**, *49*, 6789−6801.
(19) Friesner, R. A.; Banks, J. L.; Murphy, R. B.; Halgren, T. A.; Klicic, J. J.; Mainz, D. T.; Repasky, M. P.; Knoll, E. H.; Shelley, M.; Perry, J. K.; Shaw, D. E.; Francis, P.; Shenkin, P. S. *J. Med. Chem.* **2004**, *47*, 1739−1749.
(20) Halgren, T. A.; Murphy, R. B.; Friesner, R. A.; Beard, H. S.; Frye, L. L.; Pollard, W. T.; Banks, J. L. *J. Med. Chem.* **2004**, *47*, 1750−1759.
(21) *MACCS-II*; MDL Information Systems/Symyx: Santa Clara, CA, 1984.
(22) Sastry, M.; Lowrie, J. F.; Dixon, S. L.; Sherman, W. *J. Chem. Inf. Model.* **2010**, *50*, 771−784.